Primljen / Received: 22.1.2019.
Ispravljen / Corrected: 25.3.2019.
Prihvaćen / Accepted: 8.5.2019.
Dostupno online / Available online: 10.3.2020.

Damage index for reinforced concrete columns

Authors:

Mounir Ait Belkacem, PhD. CE
National Earthquake Engineering Research Centre, Algeria
ait_belkacem1@yahoo.fr
Autor za korespodenciju

Prof. **Hakim Bechtoula**, PhD. CE
National Earthquake Engineering Research Centre, Algeria
bechhakim@gmail.com

Prof. **Nouredine Bourahla**, PhD. CE
Ecole Nationale Polytechnique, Algeria
Civil Engineering Department
Laboratory LGSDS
nedbourahla@gmail.com

Adel Ait Belkacem, MCE
Bab Ezzouar University of Science & Technology, USTHB
Adel.AitBelkacem@keller-algerie.com

Research Paper

Mounir Ait Belkacem, Hakim Bechtoula, Nouredine Bourahla, Adel Ait Belkacem

Damage index for reinforced concrete columns

Severe earthquake ground motions can cause various levels of damage to reinforced concrete structures. Among others, damage index (DI) is a reliable means to quantitatively measure the extent of damage that can be endured by a structure in such circumstances. This paper outlines available concepts with a view to propose a new concept taking into account the displacement ductility of specimens loaded under low rotation angles or subjected to low fatigue test. The proposed DI has been successfully applied to predict damage levels in several case studies.

Key words:
reinforced concrete structures, earthquake, damage index, displacement ductility

Prethodno priopćenje

Mounir Ait Belkacem, Hakim Bechtoula, Nouredine Bourahla, Adel Ait Belkacem

Indeks oštećenja armiranobetonskih stupova

Jaki seizmički pomaci tla mogu uzrokovati različite razine oštećenja armiranobetonskih građevina. Indeks oštećenja (DI) jedan je od pouzdanih načina za kvantitativno mjerenje razine oštetljivosti koju građevine mogu izdržati u takvim okolnostima. U ovom se radu prikazuju postojeći koncepti te se predlaže novi koncept u kojem se u obzir uzima duktilnost s obzirom na pomak uzoraka opterećenih pri malim kutovima zaokreta ili u pokusu niskocikličnog zamora. Predloženi DI uspješno je primijenjen za predviđanje razine oštećenja u okviru nekoliko primjera, slučajeva.

Ključne riječi:
armiranobetonske građevine, potres, indeks oštećenja, duktilnost s obziorm na pomak

Vorherige Mitteilung

Mounir Ait Belkacem, Hakim Bechtoula, Nouredine Bourahla, Adel Ait Belkacem

Schadensindex von Stahlbetonsäulen

Starke seismische Verschiebungen des Bodens können Stahlbetongebäude unterschiedlich stark beschädigen. Der Schadensindex (DI) ist eine zuverlässige Methode für eine quantitative Messung des Schadensniveaus, dem ein Gebäude unter solchen Umständen standhalten muss. In dieser Abhandlung werden bestehende Konzepte dargestellt sowie ein neues Konzept vorgeschlagen, in dem die Duktilität in Bezug auf die Verschiebung der Proben berücksichtigt wird, die bei niedrigen Drehwinkeln oder im Ermüdungsexperiment mit geringem Zyklus belastet werden. Das vorgeschlagene DI wurde für die Vorhersage des Schadensniveaus im Rahmen einiger Fallstudien erfolgreich angewendet.

Schlüsselwörter:
Stahlbetongebäude, Erdbeben, Schadensindex, Duktilität in Bezug auf die Verschiebung

1. Introduction

Several research works have addressed the issue of damage indices in an attempt to classify seismically induced damage. These can be categorized in three classes as follows [1-4]:
a) *Local damage indices:* For cyclic loading, damage indices are cumulative and depend on the motion waveform and the number of excursions, but can also be non-cumulative for non-cyclic loading.
b) Global damage indices: characterize the entire structure by using combinations of local damage indices. They are determined by summing weighted local indices or by assessing variation of modal properties of the damaged structure;
c) *Individual damage indices:* denote a component of the structure or individual element of the structure.

Currently available concepts regarding DIs can be divided into two distinct classes – cumulative DIs and non-cumulative DIs. The latter are generally simple but often they do not reflect the state of damage accurately due to non-inclusion of cyclic loading effects. On the other hand, cumulative DIs are more coherent but relatively more complicated than the non-cumulative DIs as they do include the effects of cyclic loading. The following sections will review available DIs to date and will briefly address their significance.

Non-cumulative damage indices

The simplest available DI is the ductility ratio, which is expressed as the ratio of the maximum deformation u_m in loading time history to the yield displacement u_y. This concept produces damage indices varying from 0 to 1 when a structure works in the region before yielding and exceeds 1 when the structure goes into the plastic range after yield; i.e., there is no upper limit to define the state of collapse.
Lateral displacement is one of the most common parameters that can be used to define the extent of damage in a structure. This concept expresses DI as the ratio of the maximum relative lateral displacement Δu of a storey or a building to the height of that particular storey or building h. This ratio is called drift, which always produces damage indices with magnitudes much smaller than 1.
Drift can be divided into two types - transient drift and permanent drift. Both types of drift are closely related to the state of damage of a structure and hence are often used to evaluate damage levels of a structure. The following guidelines are available in FEMA 356 (ASCE, 2000) to identify the damage state of a structure [5]:

- Very light damage (operational): No permanent drift can be observed. The original stiffness and strength of the structure are retained although individual elements may exhibit minor cracking.
- Light damage (immediate occupancy): Transient drift < 1 % and no or negligible permanent drift.
- Moderate (life safety): Transient drift < 2 % and permanent drift < 1 %. Residual strength and stiffness remain in the structure but the building may be economically irreparable.
- Severe damage (collapse prevention): Transient or permanent drift < 4 %.

In addition to the drift, FEMA 356 (ASCE, 2000) defines different performance levels – Immediate Occupancy (IO), Life Safety (LS) and Collapse Prevention (CP) based on the use of plastic hinge capacity.
In 1981, the damage of concrete frame buildings was analysed and the DI was expressed as the ratio of initial stiffness to the reduced secant stiffness at maximum displacement. This model ignores tension cracks and produces a value of 0 at yielding, whilst generating a DI of 1 as the structure reaches its maximum displacement.
Also, the seismic damage to RC members was investigated and a DI based on the flexibility of a structure proposed, which was later modified as given in Eq. (1) [6-8].

$$DI = \frac{f_m - f_0}{f_u - f_0} \tag{1}$$

where, f_o is the pre-yield flexibility, f_m is the secant flexibility at a given load, and fu is the secant flexibility at ultimate load. However, this model has the same limitations as the one proposed by Roufaiel and Meyer [6].
In recognition of the changing fundamental period (T) as structures experience different states of damage due to seismic excitation, an index called "final softening" was proposed, which was later exploited to define the DI as shown in Eq. (2). The changing fundamental period was later employed in damage model [9-11].

$$DI = 1 - \left[\frac{T_{initial}}{T_{final}} \right]^2 \tag{2}$$

where, $T_{initial}$ is the fundamental period of the first step and T_{final} is the fundamental period of the last step. A similar technique was adopted but it replaced the fundamental period terms by the stiffness parameters of the structure to assess the extent of damage. Eq. (3) shows formulation for the i-th storey, whilst Eq (4) gives DI for the entire frame [9, 10, 12]:

$$DI = 1 - K^i_{final} \,/\, K^i_{initial} \tag{3}$$

$$DI = 1 - K_{final} \,/\, K_{initial} \tag{4}$$

The Seismic damage is predicted by a deterministic approach and deformations are used to propose Eq. (5) to calculate DI, where um is the maximum deformation, u_y is the yield deformation

and u_u is the ultimate deformation under monotonic load. It is worth noting that the process of collapse can be clarified as: onset of collapse, near collapse (progressing towards collapse), and total collapse. The ultimate deformation u_u is defined as the deformation at the onset of collapse; therefore, um is larger than u_u when a structure is in the near collapse and total collapse situations. The limitation of Eq. (5) is that DI becomes negative when the structure works in the region before yielding and DI exceeds 1 when the structure is beyond the onset of collapse [13].

$$DI = \frac{u_m - u_y}{u_u - u_y} \tag{5}$$

A concept for DI combining the flexural DI (D_{fl}) and shear DI (D_{sh}) of a structure has recently been proposed as shown in Eq.(6) [14]:

$$DI_{tot} = 1-\left(1-D_{fl}\right)^{\alpha} .\left(1-D_{sh}\right)^{\beta} \tag{6}$$

where, α and β are exponents related to the relative importance of D_{fl} defined in Eq.(7) and D_{sh} defined in Eq. (8) to the total damage index DI_{tot}. Also, it is propsed to assume α = β = 1. Eq. (9) shows a modified version of the total DI including the individual effects of flexure and shear [14].

$$D_{fl} = 1-\left(1-\frac{\varphi_{max}-\varphi_0}{\varphi_u-\varphi_0}\right)^{\xi} \tag{7}$$

$$D_{sh} = 1-\left(1-\frac{\gamma_{max}-\gamma_0}{\gamma_u-\gamma_0}\right)^{\rho} \tag{8}$$

$$D_{tot} = 1-\left(1-\frac{\varphi_{max}-\varphi_0}{\varphi_u-\varphi_0}\right)^{\xi}\cdot\left(1-\frac{\gamma_{max}-\gamma_0}{\gamma_u-\gamma_0}\right)^{\rho} \tag{9}$$

where, φ_{max} is the maximum curvature, φ_u is the curvature capacity and is the threshold value of curvature, while γ_{max} is the maximum shear distortion, is the shear distortion capacity and is the threshold value for shear distortion. ξ and p and are parameters for the flexural deformation ratio and shear deformation ratio respectively. Assuming that they are equally important i.e., ξ = p their proposed DI may be expressed as shown in Eq. (10).

$$D_{tot} = 1-\left(1-\frac{\varphi_{max}-\varphi_0}{\varphi_u-\varphi_0}\right)^{\xi}\cdot\left(1-\frac{\gamma_{max}-\gamma_0}{\gamma_u-\gamma_0}\right)^{\xi} \tag{10}$$

The assumption, according [9-11], of φ_0=γ_0=0 was used in their study. This results in damage indices larger than 0 for any small elastic deformation. If and correspond to yielding values, the curvature ratio of Eq. (7) and the shear distortion ratio of Eq. (8) are very similar to the deformation ratio of Eq. (5), where deformation is separated into curvature and shear distortion.

Cumulative damage indices

Under cyclic loading or earthquake ground motions, cumulative damage models are more appropriate for evaluating the damage level of structures. A trend to address the issue is to use a parameter that relates to damage and is cumulative during the loading time. In a simple way, a DI can be expressed in terms of cumulative damage as the sum of inelastic rotations during half cycles to the yield rotation [15].

Eq. (11) proposes a DI based on deformation and hysteretic energy due to an earthquake action [16].

This definition of DI is straightforward and simple, and is therefore widely used and can be applied to most cases to provide distinct damage levels [10]. It can be formulated as follows:

$$DI = \frac{u_m}{u_u} + \beta\frac{E_h}{F_y u_u} \tag{11}$$

where, u_m is the maximum displacement of a single-degree-of-freedom (SDOF) system subjected to earthquake, u_u is the ultimate displacement under monotonic loading, E_h is the hysteretic energy dissipated by the SDOF system, F_y is the yield force, and β is the parameter related to the repeated loading effect.

Note that DI > 0 corresponds to a structure that deforms within elastic range and DI > 1 corresponds to a collapse of a structure with no specified upper limit for DI. The damage state is classified into five levels:

DI < 0,1	No damage or localized minor cracking.
0,1 ≤ DI < 0,25	Minor damage: light cracking throughout.
0,25 ≤ DI < 0,40	Moderate damage: severe cracking, localized spalling.
0,4 ≤ DI < 1,00	Severe damage: concrete crushing, reinforcement exposed.
DI ≥ 1,00	Collapse.

DI ≥ 0.8 is proposed as the collapse status; DI is also proposed for a part of a structure (individual storey) and for the entire structure using the weighting factor based on the dissipated hysteretic energy (*Ei*) by the element or component, as shown in Eqs. (12) to (15) [15, 16]:

$$DI_{storey} = \sum_{i=1}^{n}\left(\lambda_{i,component}.DI_{i,component}\right) \tag{12}$$

$$\lambda_{i,component} = \left[\frac{E_i}{\sum_{i=1}^{n}E_i}\right]_{component} \tag{13}$$

$$DI_{overall} = \sum_{i=1}^{n}\left(\lambda_{i,storey}.DI_{i,storey}\right) \tag{14}$$

$$\lambda_{i,storey} = \left[\frac{E_i}{\sum_{i=1}^{n} E_i} \right]_{storey} \quad (15)$$

The concept of Park and Ang's [16] has been adopted by several researchers and a number of proposed modifications are briefly discussed herein. The most significant modification replaced the deformation terms by the moment-rotation behaviour and deducted the non-permanent or recoverable rotation, as shown in Eq. (16) [16-18]:

$$DI = \frac{\theta_m - \theta_r}{\theta_u - \theta_r} + \beta \frac{E_h}{M_y \theta_u} \quad (16)$$

where, θ_m is the maximum rotation in loading history, is the ultimate rotation capacity, θ_r is the recoverable rotation when unloading, and M_y is the yield moment. The advantage of this development is that DI is equal to 0 when structures deform within an elastic range. However, the proposal does not resolve the fact that the DI > 1 when the structure fails.

Some other modified versions of Park and Ang's [16] model, quite similar to the original model, have also been proposed. It is worth noting that Park and Ang model is still widely used by researchers although it was proposed in 1985 [19-24]. Stephens [25] proposed a DI based on the theory of low-cycle fatigue to analyse the damage of structures subjected to seismic load [25]. The calibration of the proposed DI is relatively complicated, i.e. it is related to the whole response history of structures but does not include the effects of plastic deformation proposed in Eq. (17) considering a similar approach following the rules of low-cycle fatigue. The major limitation of this proposal is that the DI becomes negative when the structure works in the region before yield and DI > 1 when the structure fails [12, 26].

$$DI = \frac{u_m - u_y}{u_u - u_y} \frac{1}{1 - \frac{E_h}{4(u_u - u_y)F_y}} \quad (17)$$

The damage level the structure can endure is closely related to the quantity of energy dissipated by the structure. Therefore, the DI may be defined as the ratio of the hysteretic energy demand (E_h) to the energy dissipation capacity of a structure under monotonic loading (E_{hu}) [27, 29]. Obviously, such a definition of DI leads to no specific upper limit that would characterize the state of collapse. The absorbed energy is also used to define damage indices, as shown in Eq. (18) [30].

$$DI = (2-b)\frac{aNE_h}{2r(\mu_u - 1)} \quad (18)$$

where *a* is the structural parameter that accounts for the energy content of the ground motion; *b* is the structural parameter that characterises stability of the hysteretic cycle; *r* is the reduction factor that characterises the cyclic deformation capacity of a system; $\mu_u = u_u/u_y$ is the ultimate ductility capacity; $NE_h = E_h/F_y u_y$ is the normalised hysteretic energy. The parameter *b* varies from 1.5 to 1.8. The value *b* = 1.5 was used for the seismic design of ductile structures. In this case, Eq. (18) can be re-writen as Eq. (19) [31].

$$DI = \frac{aE_h}{r\left[4(u_u - u_y)F_y\right]} \quad (19)$$

The term $4(u_u - u_y)F_y$ is the energy of an ultimate complete cycle in the case of an elastic perfectly- plastic state. In general, Eq. (19) is basically the ratio of the hysteretic energy demand to the energy of one ultimate complete cycle (can be understood as energy capacity).

However, the incorporation of two factors: *a* for energy demand, (E_h) and *r* for energy capacity makes the damage index equal to 1 when the structure collapses. According to the authors, the damage model suffers from two issues: harmonization of definitions used and results obtained by researchers, and clear understanding of the damage model applied for the design of a particular structure [30]. Using the damage indices found for chosen specimens, and taking into account the results of the low cycle fatigue test, a new formulation of the coefficient βe is proposed in this paper.

Finally, the correlation between damage indices and damage states for all specimens is investigated.

2. Performance of circular columns under fatigue test

The test consisted of testing 12 circular bridge piers under different loading paths. Only 6 specimens were used in this section. These data were taken from the Database compiled by M.O. Eberhard at the University of Washington. Table 1 compares the prototype to the model [32].

Two specimens were used for benchmark testing: the first specimen was loaded monotonically and unidirectionally up to failure, and the second specimen was subjected to a standard quasi-static cyclic load. Four specimens were tested for fatigue characteristics under constant amplitude cycling.

2.1. Design of model specimen

A quarter scale model, for which no special modelling treatment was necessary, was selected as an appropriate size. Only dimensional scaling was used. Table 1 shows the dimensions, reinforcement details, concrete strength, axial load applied, and lateral load capacity for both the prototype and the model.

The details of load frame, test set-up, and arrangement of reinforcement, are shown in Figure 1.

The complete set of experiments showing the type of imposed displacement is presented in Table 2.

Table 1. Comparison between the prototype and model

Item	Prototype	Model	Remarks
Longitudinal reinforcement	24#11 (36 mm)	21#3 (9.5 mm)	ρ = 2 %
Spirals	#5 (16 mm)	Wire 4 mm diameter	Smooth wire
Spiral pitch	76 mm	19 mm	ρv = 0.1
Spiral yield	414 MPa	380 to 450 MPa	-
Column diameter	1220 mm	305 mm	1/4 scale
Concrete strength	/	Specimen: 1.2.3 : 29 MPa Specimen: 4.5.6 : 35.5 MPa	/
Column length	5500 mm	1372 mm	1/4 scale
Cover	50 mm	12.5 mm	1/4 scale
Axial load	3225 kN	806 kN	
Lateral load capacity	1550 kN	388 kN	/
Spacing of long. steel	100 mm	25 mm	/

Table 2. Displacement histories used in testing

Specimen	Load routine	Direction X, Load history	Direction Y, Load history	Plan view of load
1	Monotonic pushover test			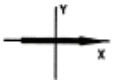
2	Standard displacement pattern			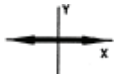
3	2 Δy to failure	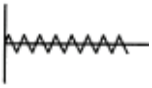		
4	3 Δy to failure	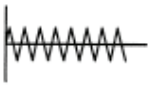		
5	4 Δy to failure	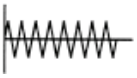		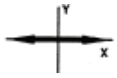
6	5 Δy to failure			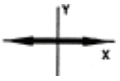

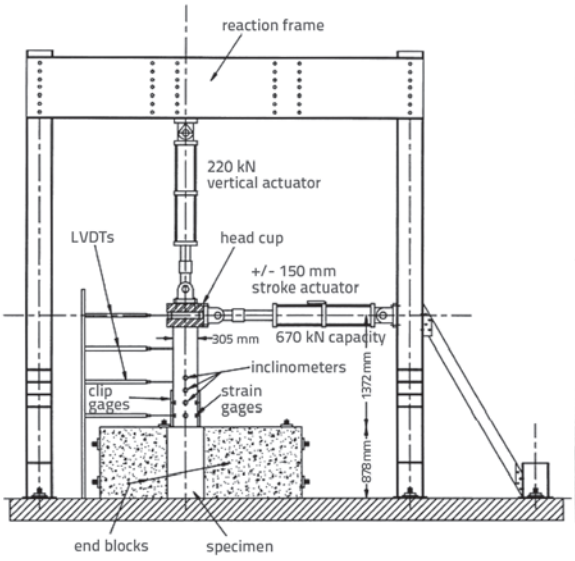

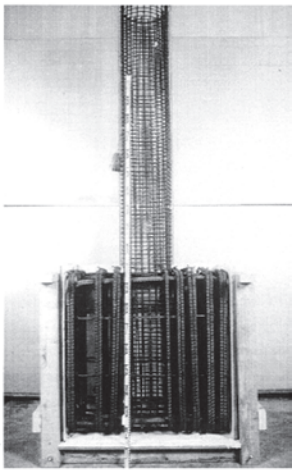

Figure 1. Details of load frame, test set-up and arrangement of reinforcement

2.3. Relation between rotation angle and dissipated energy

Specimen 1 was monotonically loaded (pushover) until failure. Specimen 2 was loaded with 3 cycles at each of the following prescribed rotation angles: 1.0 %, 1.5 %, 2.0 %, 2.5 %, 3.0 %, 4.0 %, 5 % and 6 %. Specimens 3, 4, 5, and 6 were loaded until failure at a constant rotation angle of 2.0 %, 4.0 %, 5.5 %, and 7.0 %, respectively, as shown in Table 3. The rotation angle is defined as the ratio of the column top displacement divided by the height of the column.

Table 3. Summary of the loading types and number of cycles until failure

Specimen	Rotation angle [%]	No. of cycle until failure
1	Monotonic	/
2	Standard	24
3	2.0	400
4	4.0	26
5	5.5	10
6	7.0	5

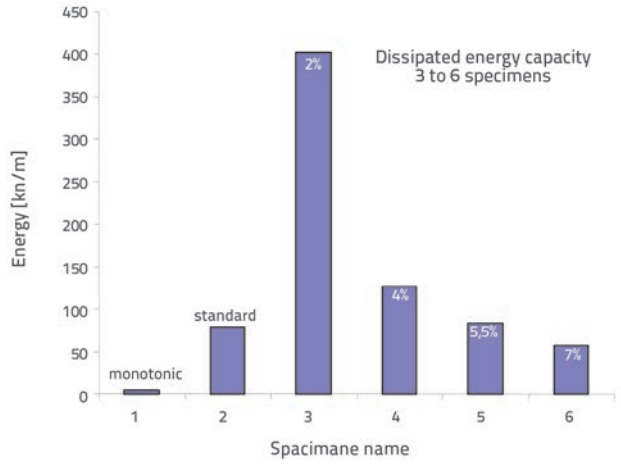

Figure 2. Dissipated energy in six specimens

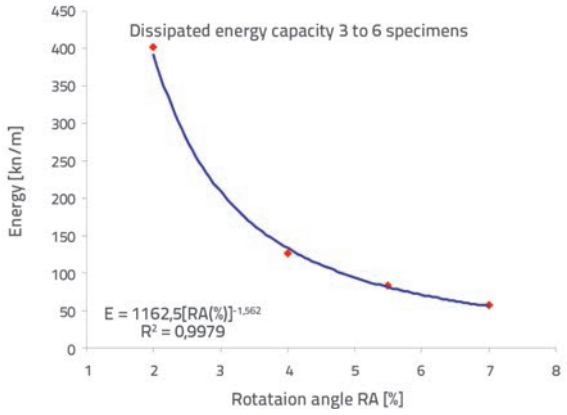

Figure 3. Relation between dissipated energy and rotation angle

Figure 2 shows the dissipated energy in six specimens. It can be seen that the energy dissipated under monotonic loading is very low compared to that of the cyclic loading. The dissipated energy for specimen subjected to standard cyclic loading was in between those of specimens tested at 4 to 7 % constant rotation angles. As can clearly be seen in Figure 3, the dissipated energy capacity decreases with an increase in the constant rotation angle. The following formulation, relating the dissipated energy (E) to the rotation angle (RA) in percent, was found by regression analysis with a correlation coefficient of 99.8 %:

$$E(kNm) = 1162{,}5\,[RA(\%)]^{-1{,}562} \quad (20)$$

2.4. Relation between rotation angle and number of cycles until failure

The number of cycles until failure is shown for each specimen in Figure 4. The number of cycles to failure is expected to decrease rapidly with an increase in deformation, from 2 % to 4 % rotation angles, and to decrease gradually nearly in a linear manner in the range of 4 % to 7 % rotation angles. Based on regression analysis, the number of cycles until failure, N_f, can easily be determined using Eq. 21, the coefficient of correlation was 99.4 %:

$$N_f = 4206{,}2\,[RA(\%)]^{-3{,}528} \quad (21)$$

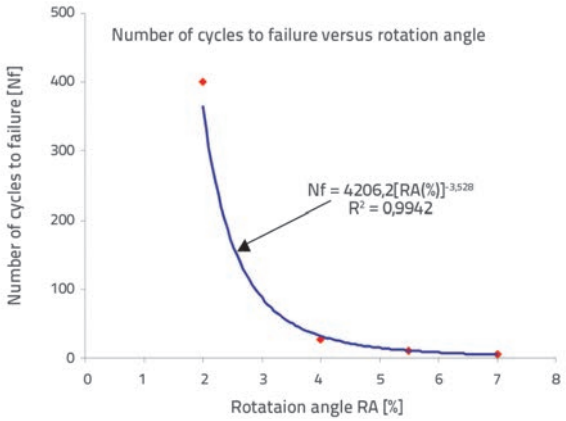

Figure 4. Relation between the number of cycles until failure and rotation angle

A method for predicting the dissipated energy for an identical specimen tested under any kind of loading history is proposed using benchmark results for specimens 3 to 6. In our case, specimen 2 was chosen to verify the proposed procedure. Since specimen 2 was loaded at a rotation angle different from that of benchmark specimens, Eq. 20 and Eq. 21 were used to determine the dissipated energy and the number of cycles until failure for fictitious specimens loaded to the same constant drift angle as specimen 2. The results of the procedure are summarized in Table 4. In this testing, the computation started from the rotation angle of 1.5 % because the yielding rotation angle for specimen 2 was, δ_y = 1,33 %. The dissipated energy of a considered specimen (E) can be written as a function of the dissipated energy by the benchmark specimens, in the following form:

$$E = \sum_i \frac{N_i}{Nf_i} Ef_i \quad (22)$$

Table 4. Results of fictitious specimens

Rotation angle [%]	N_f (calculated)	N_f (used)	Energy [kN.m] (calculated)	Energy [kN.m] (used)
1.5	1006.10	1006	617.08	617.08
2.0	364.63	400	393.72	402.53
2.5	165.94	166	277.85	277.85
3.0	87.22	88	208.99	208.99
4.0	31.61	26	133.34	125.86
5.0	14.39	15	94.10	94.10
6.0	7.56	8	70.78	70.78

where: N_i is the number of cycles of the considered specimen for a rotation angle N_{fi} and E_{fi} are the number of cycles and the dissipated energy of the benchmark specimen loaded under a constant rotation angle i, respectively. In our case, specimen 2 was loaded with 3 cycles for each prescribed rotation angle, hence $N_i = 3$.

Applying Eq. (22) to specimen 2, it was established that the dissipated energy is E_{eq} = 76.9 kNm.This result represented 97 % of the dissipated energy of specimen 2 found directly from the test, E_{test} = 79.3 kNm. Hence, the energy dissipated by a specimen tested under any kind of cyclic loading can easily be evaluated if the energy-rotation angle and the number of cycles to failure versus the rotation angle curves are known.

The damage index (DI) for specimen 2 was also evaluated using the number of cycles to failure of benchmark specimens. Miner's linear rule is expressed as:

$$D = \sum_i \frac{N_i}{N_{fi}} \qquad (23)$$

Value N_i and N_{fi} are the quantities introduced earlier. The damage value of DI = 0.75 for specimen 2, corresponding to a severely damaged state, is given in Eq. (23). This value is consistent with the observed damage [33]. That is summarized as follows:

- Yielding took place at around 20 mm displacement corresponding to 1.4 % rotation angle.
- Spalling of concrete cover was observed at a drift of 3 %.
- Crack propagated until a height of 225 mm corresponding to 0.74 of the column diameter.
- Minor buckling was observed at the rotation angle of 4 %.
- Failure of the specimen occurred at the rotation angle of around 6 %, following rupture of the spiral in the plastic hinge region.

The damage progress for specimen 2, tested under a standard loading history, is shown in Figure 5. The maximum analytical damage index, computed using Park et al. model, amounted to 0.94, which is near the collapse state according to the damage classification given by Park [16]. The analytical damage indices for specimens 5 and 6 at the end of cyclic loading were 0.96 and 0.94, respectively, as shown in figures 6 and 7. These values accurately reflect the damage state of the specimens that were near the collapse at the end of the test.

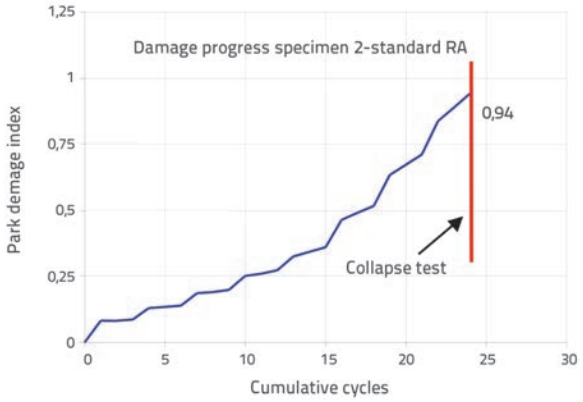

Figure 5. Damage progress for specimen 2

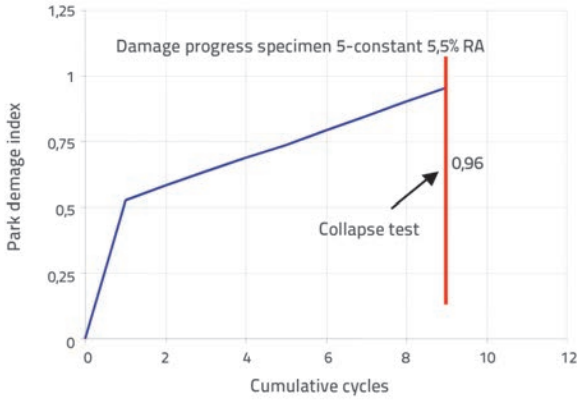

Figure 6. Damage progress for specimen 5

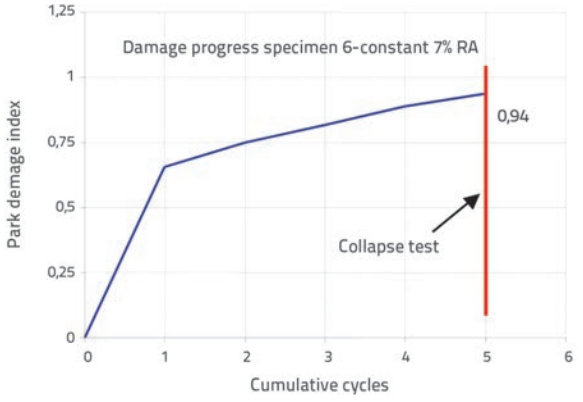

Figure 7. Damage progress for specimen 6

3. Proposed damage index

It should be noted here that the damage index proposed by Park et al. overestimated the damage state of specimens 3 and 4 as shown in figures 8 and 9. After 150 cycles, specimen 3 still supported the applied load without any degradation. The computed damage index at that state was 1.0, which corresponds to failure according to Park's classification. At the end of the test, failure state, the Park et al.'s damage index was 2.49 for specimen 3 loaded with a constant 2 % rotation angle and 1.10 for specimen 4 loaded with 4 % rotation angle until failure.

In this case, we suggest that the damage index proposed by Park et al be modified in order to take into account the fatigue phenomena. This can be done by modifying the ß factor included in the Damage Index Park formula. Also, the new formulation will take into account the loading path history.

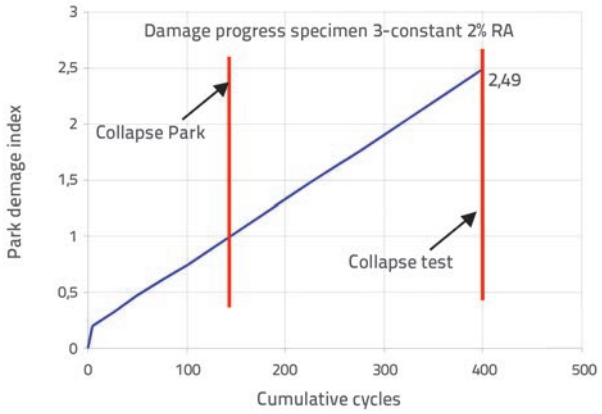

Figure 8. Damage progress for specimen 3

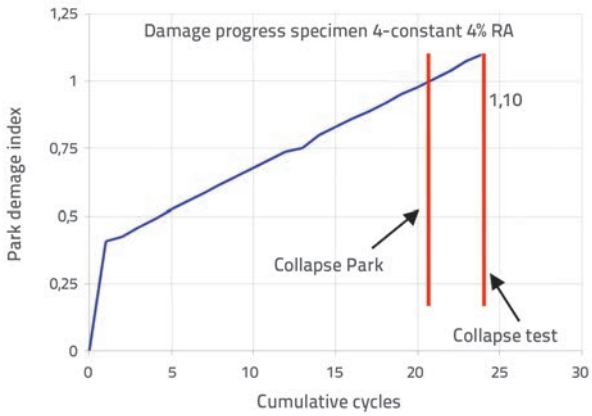

Figure 9. Damage progress for specimen

This shows that Park et al.'s damage model may overestimate the damage index for specimens loaded under low rotation angles or low fatigue test, as illustrated in Figure 10.

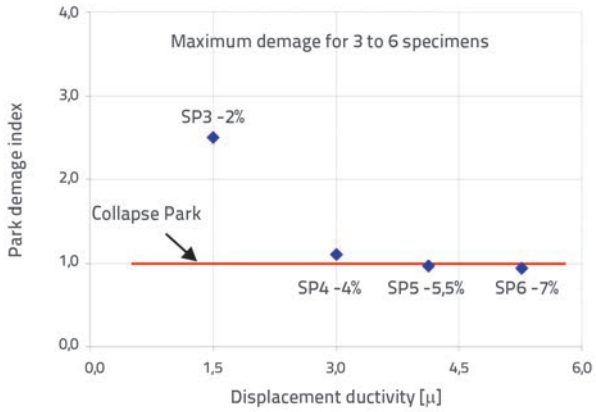

Figure 10. Summary of computed Park et al. damage index

A new formulation of the β_e coefficient that takes into account the results of the low cycle fatigue test is proposed using the damage indices determined for specimens 3 and 4.

Since the maximum damage that can be reached is limited to D_I=1,0, the following Eq. (24) can be used:

$$D_I = \frac{\delta_m}{\delta_u} + \beta'_e \frac{\int dE}{\delta_u F_y} \tag{24}$$

where: β'_e is the value that corresponds to the limit damage state of D_I=1,0. We can determine β'_e as:

$$\beta'_e = \beta_e - \frac{D_i - D_I}{\int dE / (\delta_y F_y)} \tag{25}$$

As illustrated in Figure 11, reduction of β_e must be taken into account for displacement ductilityμ ≤ 3,41. This value represents the intersection of the ascending branch and the constant branch in the β_e-μ relationship.

With respect to displacement ductility, the new β_e formulation can be written as follows:

$$\begin{aligned} \beta_e &= 0{,}0167\mu - 0{,}007 \quad \text{for } \mu \le 3{,}41 \\ \beta_e &= 0{,}05 \quad \text{for } \mu > 3{,}41 \end{aligned} \tag{26}$$

However, more investigation and tests are needed to improve this formulation. For this, eleven (11) specimens subjected to cyclic loading were selected in the following section and the DI improvement formulation was applied and compared with damage states of specimens during experimental tests.

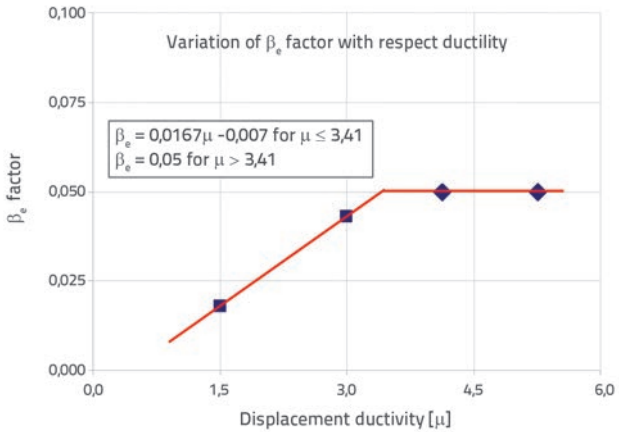

Figure 11. Proposed curve for β_e variation

4. Damage analysis: Application

In this section, the damage index (DI) is calculated using the proposal formulation given in Eq. (24). For this purpose, eleven (11) specimens subjected to cyclic loading were carefully selected from the database compiled by M.O. Eberhard at University of Washington, as shown in Table 5. The correlation between damage indices and damage states for all specimens was investigated as shown in Table 6 [34-37].

The computed damage matched well the damage observed during the test for all specimens, as illustrated in Table 6. It can be observed that, for specimens that suffered some buckling of the longitudinal reinforcement, the computed damage index provide a numerical value greater than 0.8.

Table 5. Geometric characteristics, loading and reinforcement ratios of selected columns

Specimen	fc [MPa]	Axial load [kN]	Geometric characteristics				Reinforcement ratios	
			B [mm]	H [mm]	L [mm]	Configure	Longitudinal	Transversal
01	44	2112	400	400	1600	DE	0.0150	0.012
02	44	2112	400	400	1600	DE	0.0150	0.008
03	41	3280	400	400	1600	DE	0.0150	0.007
04	40	3200	400	400	1600	DE	0.0150	0.003
05	34	1782	350	350	1645	C	0.0190	0.01
06	34	1782	350	350	1645	C	0.0190	0.02
07	39	4368	400	400	1600	DE	0.0150	0.007
08	34	831	350	350	1645	C	0.0190	0.02
09	25.3	450	400	400	1400	C	0.0210	/
10	27.1	675	400	400	1400	C	0.0210	/
11	26.8	900	400	400	1400	C	0.0210	/

DE - double ended; C - Cantilever
Observations: The damage observed during experimental tests (crushing of concrete and buckling of rebars) is given at the corresponding displacement [32].

Table 6. Observed damage and computed damage index

Experimental results [32]			Analytical results		
Specimen	Crushung [mm]	Long bar buckling [mm]	Proposal damage indexi (DI)	Classification	
01	34.2	68.4	0.88	D > 0.8	Collapsed of column
02	30.6	44.9	0.85		
03	18.5	0	0.79	0.4 < D < 0.8	Extensive crushing of concrete
04	18.5	0	0.69		
07	12.3	0	0.70		
05	32.9	0	0.51		
06	32.9	82.3	0.83	D > 0.8	Collapsed of column
08	32.9	0	0.79	0.4 < D < 0.8	Extensive crushing of concrete
09	42.5	0	0.78		
10	37	104	0.92	D > 0.8	Collapsed of column
11	36	111	0.95		

5. Conclusion

A review of available damage index concepts was presented in this paper. Park and Ang [16] proposed their DI considering changes in both deformation and energy during an earthquake; this is the most widely accepted concept to date. The major drawbacks are that it gives a positive number even when a structure is still within the elastic range, and that there is no upper limit for DI, i.e. results tend to get erratic in nature when a structure approaches collapse. Park et al.'s damage model may overestimate the damage index for specimens loaded under low rotation angles or based on low fatigue test. The proposed concept includes a modified formulation of the coefficient that takes into account the results of the low cycle fatigue test and displacement ductility. The Damage Index improvement satisfies the essential characteristics for an appropriate damage model and produces rational values of damage indices. However, further research should be conducted to validate this approach due the limited number of analysed specimens.

REFERENCES

[1] Kappos, A.J., Stylianidis, K.C., Michailidis, C.N., Athanassiadou, C.J.: Development of Earthquake Damage Scenarios using a Comprehensive Analytical Method. Proc. of the 10th World Conf. on Earthquake Engng, 10 (1992), pp. 6013-6018.

[2] Mieses, H.L.A.: Seismic Performance and Fragility Curves for Reinforced Concrete Frames and Shear Wall Residential Buildings in Puerto Rico, PhD. Thesis, Univ of Puerto Rico, 2007.

[3] Golafshani, A.A., Bakhshi, A., Tabeshpour, M.R.: Vulnerability and Damage Analysis of Existing Buildings, Asian Journal of Civil Engineering, 1 (2005) 6, pp. 85-100.

[4] Williams, M.S., Sexsmith, R.G.: Seismic Damage Indices for Concrete Structures: A State-of-the-Art Review. Earthquake Spectra, 11 (1995) 2, pp. 319-349.

[5] ASCE, Prestandard and commentary for the seismic rehabilitation of buildings, Prepared for Federal Emergency Management Agency, FEMA Publication No. 356. Washington, D.C.: Federal Emergency Management Agency, 2000.

[6] Roufaiel, M.S.L., Meyer, C.: Analysis of damaged concrete frame buildings. Technical Report No. NSF-CEE-81-21359-1, Columbia University, New York.1981.

[7] Banon, H., Biggs, J.M., Irvine, H.M.: Seismic damage in reinforced concrete members. Journal of Structural Engineering, 107 (1981) 9, pp. 1713–1729.

[8] Roufaiel, M.S.L., Meyer, C.: Analytical modeling of hysteretic behavior of R/C frames. Journal of Structural Engineering, ASCE, 113 (1987) 3, pp. 429–444.

[9] DiPasquale, E., Ju, J.W., Askar, A.: Relation between global damage indices and local stiffness degradation, Journal of Structural Engineering, 116 (1990) 5, pp. 1440-1456.

[10] Kim, T.H., Lee, K.M., Chung, Y.S.: Seismic damage assessment of reinforced concrete bridge columns. Engineering Structures, 27 (2005), pp. 576–592.

[11] Massumi, A., Moshtagh, E.: A new damage index for RC buildings based on variations of nonlinear fundamental period, The Structural Design of Tall and Special Buildings, 2010.

[12] Ghobarahn, A., Abou-Elfath, H., Biddah, A.: Response-based damage assessment of structures. Earthquake Engineering & Structural Dynamics, 28 (1999), pp. 79-104.

[13] Powell, G.H., Allahabadi, R.: Seismic damage prediction by deterministic methods: Concepts and procedures. Earthquake Engineering & Structural Dynamics, 16 (1988), pp. 719-734.

[14] Mergos, P.E., Kappos, A.J.: Seismic damage analysis including inelastic shear–flexure interaction. Bulletin of Earthquake Engineering, 8 (2009), pp. 27-46.

[15] Banon, H., Veneziano, D.: Seismic safety of reinforced members and structures. Earthquake Engineering & Structural Dynamics, 10 (1982) 2, pp. 179-193.

[16] Park, Y.J., Ang, A.H.S.: Mechanistic seismic damage model for reinforced concrete. Journal of Structural Engineering, 111 (1985) 4, pp. 722-739.

[17] Tabeshpour, M.R., Bakhshi, A., Golafshani, A.A.: Vulnerability and damage analyses of existing buildings, 13th World Conference on Earthquake Engineering, 2004.

[18] Kunnath, S.K., Reinhorn, A.M., Lobo, R.F.: IDARC Version 3.0: A Program for the Inelastic Damage Analysis of Reinforced Concrete Structures, Report No. NCEER-92-0022, National Center for Earthquake Engineering Research, State University of New York at Buffalo, 1992.

[19] Fardis, M.N., Economu, S.N., Antoniou, A.N.: Damage measures and failure criteria - Part I, Contribution of University of Patras Final Report of Cooperative research on the seismic response of reinforced concrete structures - 2nd Phase, 1993.

[20] Ghobarah, A., Aly, N.M.: Seismic reliability assessment of existing reinforced concrete buildings. Journal of Earthquake Engineering, 2 (1998) 4, pp. 569-592.

[21] Bozorgnia, Y., Bertero, V.V.: Evaluation of damage potential of recorded earthquake ground motion. Seismological Research Letters, 72 (2001) 2, pp. 233.

[22] Bassam, A., Iranmanesh, A., Ansari, F.: A simple quantitative approach for post earthquake damage assessment of flexure dominant reinforced concrete bridges, Engineering Structures, 33 (2011), pp. 3218-3225.

[23] Ghosh, S., Datta, D., Katakdhond, A.A.: Estimation of the Park–Ang damage index for planar multi-storey frames using equivalent single-degree systems, Engineering Structures, 33 (2011), pp. 2509-2524.

[24] Yüksel, E., Sürmeli, M.: Failure analysis of one-story precast structures for near-fault and far-fault strong ground motions, Bulletin of Earthquake Engineering, 8 (2010), pp. 937–953.

[25] Stephens, J.E.: A damage function using structural response measurements, Structural Safety Journal, 5 (1985), pp. 22-39.

[26] Reinhorn, A.M., Valles, R.E.: Damage Evaluation in Inelastic Response of Structures: A Deterministic Approach, Report No. NCEER-95-xxxx, National Center for Earthquake Engineering Research, State University of New York at Buffalo, 1995.

[27] Fajfar, P.: Equivalent ductility factors, taking into account low-cycle fatigue, Earthquake Engineering & Structural Dynamics, 21 (1992), pp. 837-848.

[28] Cosenza, E., Manfredi, G., Ramasco, R.: The use of damage functionals in earthquake engineering: A comparison between different methods, Earthquake Engineering & Structural Dynamics, 22 (1993) 10, pp. 855-868.

[29] Rodriguez, M.E., Padilla, D.: A damage index for the seismic analysis of reinforced concrete members. Journal of Earthquake Engineering, 13 (2009) 3, pp. 364-383.

[30] Teran-Gilmore, A., Jirsa, J.O.: A damage model for practical seismic design that accounts for low cycle fatigue, Earthquake spectra, 21 (2005) 3, pp. 803-832.

[31] Teran-Gilmore, A., Sanchez-Badillo, A., Espinosa-Johnson, M.: Performance-based seismic design of reinforced concrete ductile buildings subjected to large energy demands, Earthquakes and Structures, 1 (2010) 1, pp. 69-91.

[32] Berry, M., Parrish, M., Eberhard, M.: PEER structural performance database user's manual (version 1.0), University of California, Berkeley, 2004.

[33] Kunnath, S.K.: Cumulative Seismic Damage of Reinforced Concrete Bridge Piers. Techn. Rep. NCEER 97-0006, State Univ. of New York, Buffalo, 1997.

[34] Soesianawati, M.T., Park, R., Priestley, M.J.N.: Limited Ductility Design of Reinforced Concrete Columns. Report 86-10, Department of Civil Engineering, University of Canterbury, Christchurch, New Zealand, March, 1986, 208 pages.

[35] Watson, S., Park, R.: Design of Reinforced Concrete Frames of Limited Ductility. Report 89-4, Department of Civil Engineering, University of Canterbury, Christchurch, New Zealand, January, 1989, 232 pages.

[36] Saatcioglu, M., Grira, M.: Confinement of Reinforced Concrete Columns with Welded Reinforcement Grids. American Concrete Institute, ACI Structural Journal, 96 (1999) 1, pp. 29-39.

[37] Mo, Y.L., Wang, S.J.: Seismic Behavior of RC Columns with Various Tie Configurations. Journal of Structural Engineering, ASCE. 126 (2000) 10, pp. 1122-1130.